1971

Knight shift and spin-lattice relaxation measurements in the phosphides with the Ti3P structure type and in the VS [subscript 1 plus or minus x] system

Denis Michael Strachan
Iowa State University

Knight shift and spin-lattice relaxation measurements in the phosphides with the Ti_3P structure type and in the $VS_{1\pm x}$ system

by

Denis Michael Strachan

A Dissertation Submitted to the
Graduate Faculty in Partial Fulfillment of
The Requirement for the Degree of
DOCTOR OF PHILOSOPHY

Major Subject: Physical Chemistry

Approved:

Signature was redacted for privacy.

In Charge of Major Work

Signature was redacted for privacy.

Head of Major Department

Signature was redacted for privacy.

Dean of Graduate College

Iowa State University
Ames, Iowa

1971

TABLE OF CONTENTS

LIST OF FIGURES

LIST OF TABLES

I. INTRODUCTION

A. Introduction to Solid State Nuclear Magnetic Resonance

Preparative techniques in high temperature chemistry have yielded many interesting compounds, especially between the early transition metals and the group III-VI elements. The structures of the new phases have in most cases been determined, but other than the crystal structure little is known about the physical and chemical properties of the solids. Most studies of the properties of the solids have been rather superficial. For instance, if a compound has metallic luster and exhibits a low electrical resistance as measured with a vacuum tube volt-ohm meter, it has generally been reported to be metallic. The research discussed here was performed with the purpose of gaining information about some basic physical and chemical properties of several metal-rich transition metal compounds. The method used to achieve this goal was nuclear magnetic resonance (NMR).

NMR has the advantage over many other types of measurements that it utilizes a microscopic probe of the sample, namely the nucleus. If a nucleus with nuclear spin is located in a metal it serves as a sensitive probe of the type of electronic wave functions at the nucleus for electrons which participate in binding and conduction. Conduction electrons with unpaired spins and with wave functions centered on a nuclear site cause a shift in the nuclear resonance frequency

from the value observed for a free ion. This shift is called the Knight shift, after its discoverer. A rather general description of the Knight shift follows.

In a metallic compound with essentially free electrons, the conduction electrons are delocalized over the solid in a conduction band. That is, the single electron wave functions have magnitudes which do not, in general, monotonically diminish as a function of distance from some point in the solid (as would the magnitude of a molecular orbital wave function, for example), but instead these wave functions are thought to vary periodically within the solid (e.g. the Bloch function). Thus the nucleus can experience magnetic coupling with many electrons. In the absence of any external or internal magnetic field, the nucleus is coupled to electrons with random orientations of the electron spins. The unpaired electrons in such a metal have energies within kT (k = Boltzmann's constant) of the Fermi energy. Fermi energies are of the order of 3 eV, and the energy interval kT is 0.03 eV at room temperature. Each energy state below this energy interval is filled with two electrons with opposing spins, and each energy state within this energy interval has a probability of being only half filled. Energy states higher than 0.5 kT above the Fermi energy are unoccupied. Only those electrons in the singly occupied states can interact with an applied magnetic field. Application of an external magnetic field causes polarization

of the electron spins and imposes a preferred direction on the spin system. This spin polarization increases the net magnetic moment coupled to the nucleus from zero (in the absence of an applied field) to some finite value. In the applied field the net magnetic moment lies along the field direction thus increasing the effective field at the nucleus. This effective field is proportional to the applied field, and the resultant shift in the NMR signal is a positive Knight shift.

Experimental results have shown that the Knight shift is more complex than envisioned above. Negative Knight shifts have been observed and can be explained only by the consideration of an additional contribution to the shift. Observation of shift values larger than expected on the basis of the magnetic susceptibility also has required an additional shift contribution.

Consideration of a system of nuclei and conduction electrons weakly coupled by the hyperfine interaction (i.e. the $\vec{I}\cdot\vec{A}\cdot\vec{S}$ term in the Hamiltonian) and an isotropic environment (i.e. the tensor $\vec{A}$ becomes the scalar, a) leads to the first contribution to the Knight shift. For this system the Hamiltonian is $\underline{H} = \underline{H}_e + \underline{H}_n + \underline{H}_{en}$ where $\underline{H}_e$ is the Hamiltonian for the weakly interacting set of electrons, $\underline{H}_n$ is the nuclear Hamiltonian and $\underline{H}_{en}$ contains the magnetic interactions between the nuclei and the electrons. Contained in

the nuclear Hamiltonian, $\underline{H}_n$, is the Zeeman energy in the static field H_o and the dipolar coupling between nuclei. The term $\underline{H}_e = g\beta\vec{S}\cdot\vec{H}$ which accounts for the Zeeman energy of the unpaired electrons at the Fermi surface and is not relevant to the nuclear resonance experiment.

Consider the case of a spin I = 1/2 nucleus. The nuclear Zeeman term, $\underline{H}_n$, is $-\gamma h\vec{I}\cdot\vec{H}$, or, in the isotropic case, $-\gamma hIH_z$. Dipolar coupling, which causes a broadening of the NMR linewidth, will be neglected in this section. The third term in the Hamiltonian is then

$$\underline{H}_{en} = -\frac{8\pi}{3}\gamma_e\gamma_n\hbar^2 \sum_{j,\ell} \vec{I}_j\cdot\vec{S}_\ell\ \delta(\vec{r}_\ell\cdot\vec{R}_j), \qquad (1)$$

where $\vec{r}_\ell - \vec{R}_j$ is the vector from the j th nucleus to the ℓ th electron. Since the electrons and nuclei are weakly interacting the wave function can be written $\psi = \psi_e\,\psi_n$. Inasmuch as a conduction electron is delocalized over the solid, its wave function is taken to be a plane wave modulated by a function containing the periodicity of the lattice. Thus ψ_e will be the product $\psi_{\vec{k}}\,\psi_s$ where ψ_s is the spin part of the function and $\psi_{\vec{k}}$ is the Bloch function

$$\psi_{\vec{k}} = u_{\vec{k}}(\vec{r})\exp(i\vec{k}\cdot\vec{r}) , \qquad (2)$$

where $u_{\vec{k}}(\vec{r})$ is a function exhibiting the periodicity of the lattice and $\exp(i\vec{k}\cdot\vec{r})$ is a plane wave dependent on the value of the wave vector, $\vec{k}$. Taking into account that contributions to the shift arise only from those electrons within an energy

interval kT of the Fermi energy and of these electrons only those with finite probability density at the nucleus (i.e. those with s-like wave functions), the shift in energy due to the interaction of the electron with the j th nuclear spin is

$$\Delta E = - \gamma_n h I_{zj} \left[\frac{8\pi}{3} < |u_{\vec{k}}(0)|^2 >^2_{E_F} \chi^s_p H_o \right], \qquad (3)$$

where $< |u_{\vec{k}}(0)|^2 >_{E_F}$ is the probability density for finding an electron with energy E_F at the position of the nucleus and χ^s_p is the Pauli spin susceptibility of the conduction electrons with s character. Since the nuclear Zeeman energy is $- \gamma_n h I_z H$, Equation 3 represents a positive shift. Thus

$$K_s = \frac{\Delta \nu}{\nu_o} = \frac{\Delta H}{H_o} = \frac{8\pi}{3} < |u_{\vec{k}}(0)|^2 >_{E_F} \chi^s_p \, . \qquad (4)$$

In the case of transition metals the electronic states at the Fermi surface have a more complex make-up and in general the electronic wave functions are combinations of wave functions with s, p and/or d character. A more general form for the total Knight shift is

$$K_{tot} = K_s + K_p + K_d + K_{orb} \, , \qquad (5)$$

where K_s is the shift described by Equation 4, K_p and K_d are shifts arising from the so-called "core polarization" by electrons with p or d character and K_{orb} is the shift arising from the field induced orbital magnetic moment of non-s conduction electrons. Core polarization arises from the interaction of non-s electrons with inner ion core s electrons in

such a way as to cause a net magnetic coupling of the nucleus with the inner core electrons. That is to say, the wave functions at the Fermi surface are, to a first approximation, combinations of hybrid wave functions formed by linear combinations of s and non-s wave functions. The s, p or s, d coupling has been observed to yield a negative contribution to the total shift (1). In metals with narrow and partially filled conduction bands the orbital shift has been observed to be quite large (1).

Thus far only nuclei with I = 1/2 in an isotropic environment have been considered. For nuclei with I > 1/2, transitions between the other spin states complicate the NMR spectrum. If the nuclear site has less than cubic symmetry there exists an electric field gradient (EFG) at the site and the electric quadrupole moment of the nucleus interacts with the EFG in the crystal. Since the EFG is produced by the arrangement of ion cores around the nuclear site, to some extent by the type of binding in the solid and, in metals, by all of the electrons in the conduction band, the quadrupole coupling is independent of the applied field. Quadrupole satellite lines are not always observed in metallic solids due to a smearing of the EFG. As long as the EFG is small no quadrupole effect is observed on the central (m = 1/2 to m = -1/2, m = spin state) transition. Axial symmetry leads to a broadening of NMR spectra. Due to the axial symmetry the

magnetic field at which resonance will occur is a function of the crystal orientation. In a powdered sample the line shape will reflect the appropriate average over all of the crystallite orientations. For the case of axial symmetry the Knight shift is represented by an isotropic shift, K_{iso}, and an axial shift, K_{ax}. The resonant frequency is

$$\nu = \nu_o\left[1 + \frac{K_{ax}(3\cos^2\theta - 1)}{1 + K_{iso}}\right], \qquad (6)$$

and K_{ax} is given by

$$K_{ax} = \frac{1}{3}(K_{\parallel} - K_{\perp}), \qquad (7)$$

where $K_{\parallel}$ and $K_{\perp}$ are the shifts at the angles 0^o and 90^o between the crystal axis and the field direction.

Presence of the conduction electrons in the solid also has an effect on the nuclear relaxation phenomenon. A relaxation phenomenon which is sometimes important in the interpretation of the Knight shift data is spin-lattice relaxation, which is discussed briefly in the following. Consider a set of nuclei in a static magnetic field and in thermal equilibrium with a lattice (i.e. a Boltzmann population of the energy levels). The spin-lattice relaxation time is a measure of how long it takes a collection of nuclei, once excited to some higher energy level by photons, to give up the energy of the photons to the lattice. In the absence of other coupling mechanisms this process might be envisioned as rather slow. An accelera-

tion of this process is provided by the conduction electrons. The spin-lattice relaxation time, T_1 is given by

$$\frac{1}{T_1} = \frac{\frac{a_o}{2} \sum_{m,n,\alpha} \langle m|I_\alpha|n\rangle \quad (E_m - E_n)^2}{\sum_m E_m^2} \tag{8}$$

where m and n are nuclear states, α is x, y and z and

$$a_o = \frac{64}{9} \pi^3 \hbar^3 \gamma_e^2 \gamma_n^2 \langle |u_k(0)|^2 \rangle_{E_F}^2 \rho^2(E_F) kT \ , \tag{9}$$

where $\rho(E_F)$ is the density of states at the Fermi surface. Again assuming the isotropic case

$$\frac{1}{T_1} = a_o \ . \tag{10}$$

Factors in a_o look like the expression for the Knight shift, K_s, Equation 4 and thus

$$T_1 \left(\frac{\Delta H}{H_o} \right)^2 = T_1 (K_s)^2 = \left[\frac{\chi_p^s}{\rho(E_F)} \right] \left[\frac{1}{\pi k T \gamma_n^2 \gamma_e^2 \hbar^3} \right] \tag{11}$$

For free electron metals T_1 is inversely proportional to the temperature and to the square of the Knight shift.

Introductions to each of the following sections will contain more specific comments pertinent to that section and draw from the general background set forth above. Additions to the general background will be added where necessary. Each section will contain its own subsections on experiment, results and conclusions.

B. Bonding Models for the Metal Rich Compounds

This section is a brief introduction to the general bonding models of the metal rich compounds of the group IV and V transition metals with the group V and VI non-metal elements. There exist in general two schools of thought on the description of these compounds. The existence of conflicting interpretations of the structural features common to a number of metal rich compounds provided some of the impetus for the research discussed here.

The search for metal rich phases between the group IV and V transition metals and group V and VI non-metals probably had its start with Biltz and co-workers (2,3). Recent and rather extensive reviews on the metal rich compounds have been published by Jellinek (4), Haraldsen (5), Hulliger (6), Rundquist (7) and Aronsson, Lundström and Rundquist (8). The appearance of the trigonal prism as a structural feature in metal rich phosphides, arsenides and silicides was noted quite early in the investigations of these systems and has been emphasized in a number of reviews (8,9). Trigonal prismatic coordination of sulfur has long been known (e.g. in the NiAs structure type) and was observed to occur in a number of metal rich sulfides by Franzen and co-workers (10,11,12,13). In a majority of these metal rich compounds the coordination number is greater than the six needed for a trigonal prism. In these cases the trigonal prism is augmented by the

positioning of metal atoms off one or more of the three rectangular faces of the trigonal prism. In many compounds more metal rich than 1:1 the group V and VI non-metals have coordination numbers as high as nine with the augmented trigonal prismatic coordination.

Chronologically, the first school of thought used the trigonal prism as a building block in the description of the metal rich phosphides and arsenides. They considered the structures to be constructed of polyhedra of hard spheres. In their view the existence of structural features are interpretable on the basis of the r_a/r_M ratio. This ratio of the anion radius to the metal radius was calculated for each polyhedron considering hard sphere contact between the central coordinated atom and the atoms at the corners of the polyhedron. Thus for a value of the ratio equal to or less than 0.414 an octahedral coordination was favored, with the trigonal prismatic and square antiprismatic coordinations occurring for the non-metal at ratios of 0.528 and 0.645, respectively. Although the proponents of this school readily admit to many exceptions and to contributions other than size, in the final interpretation of structural features the radius ratio concept is used exclusively. No relation between physical and chemical properties and structure is sought in the hard sphere interpretations. Distortions of the polyhedra, while not predicted by the hard sphere model, occur fre-

quently and are rationalized on the basis of unit cell size and short metal-metal distances. Thus Aronson and Rundquist (9) argue

> "...The way in which the prism of rhenium atoms [in Re_3B] is distorted, two rectangular faces being larger than the third one, is obviously associated with the packing of the prisms. A more uniform expansion of the prism would result in a very short distance ... between rhenium atoms in two adjacent prisms. It should be noted that the deviation of two A-B distances (2.78 and 2.73Å) from the ideal value of 2.75Å as well as the shortening of one A-A distance to 2.73Å are such as to prevent the short rhenium-rhenium distance of 2.66Å becoming still shorter. Thus, the structure of Re_3B may be regarded as a simple close-packed arrangement of nearly spherical atoms with the radii 1.37_5 and 0.85Å respectively."

This argument leaves unanswered the question of why the unit cell is not distorted or expanded to allow undistorted trigonal prisms. To this question the hard sphere model has no answer.

A more chemically satisfying model of these compounds has been forwarded by Franzen (14). This model treats atoms as atoms and not as hard spheres. Although this model cannot be used to predict structure types, which is also true of the hard sphere model, it does give a qualitative understanding of the known physical and chemical properties. This model also succeeds in the qualitative prediction of some physical and chemical properties which are as yet unobserved. It was initially proposed (14) that a delocalized, directional, covalent bonding description was consistent with the observed

properties of conductivity, brittleness and the general metallic nature of the mono-chalconides (chalcogen = sulfur, selenium and tellurium) of some transition metals. This argument will be presented here and its extension to the more metal phases will be assumed.

An important contribution to the development of this model was the observation of the persistence of trigonal prismatic coordination of chalcogens in a wide range of compounds irrespective of the metal or radius ratio. Combining the ideas of Slater (15) and Rundle (16,17), Franzen concluded that covalent binding between metal and non-metal makes an important contribution in the formation of the non-metal coordination and hence the structure of these solids.

Using Pauling's (18) empirical equation

$$D(n) = D(1) - 0.6 \log n \qquad (12)$$

where D(n) is the bond distance of an $\underline{n}$ th order bond, approximate valences of the non-metal could be calculated. Valences calculated in this manner for non-metals in trigonal prisms were greater than 3 and frequently close to 4. Earlier Rundle (16,17) had used Equation 12 to obtain bond numbers which were consistent with the formation of electron deficient, directional covalent bonds between metal atoms and oxygen, carbon or nitrogen in some monoxides, mono-carbides and mono-nitrides with the rock salt structure. Rundle pointed out that the physical properties of the rock salt type oxides,

carbides and nitrides, especially conductivity and brittleness, are consistent with electron deficient directional covalent bonding.

Slater (15) suggested that the bonding in KCl could be described as covalent while at the same time maintaining the "ionic" character of the solid. He went on to demonstrate that all solids can be described in terms of covalent interactions and provided a consistent set of atomic radii.

Franzen applied the suggestions of Slater (15) and Rundle (16,17) to the bonding by the chalcogen in trigonal prismatic coordination. He concluded that trigonal prismatic coordination of the chalcogen was the result of approximately four bonding electrons delocalized over six orbitals centered on the chalcogen. The high valences and coordinations of the chalcogen suggested the use of d orbitals by the chalcogen to form strong metal-chalcogen bonds.

In the Zr-S system sulfur has octahedral coordination in ZrS (19), trigonal prismatic coordination in $Zr_{21}S_8$ (12), and square antiprismatic coordination in Zr_9S_2 (20). Here the hard sphere model provides no explanation since the radius ratio remains constant for the series. However, qualitatively a series such as this may be more readily understood by the filling of bonding and antibonding energy states. For instance an argument might be made that the addition of zirconium and presumably the addition of d states stabilizes

coordinations for sulfur which require the use of electronic configurations other than the ground state configuration (s^2p^4) by sulfur.

NMR, as mentioned earlier, provides a very sensitive probe of the solid state material. However, the probes must be present in sufficient number to make an experiment feasible. Sulfur in this respect is a poor probe, since the isotope with nuclear spin has a natural abundance of 0.76%. Phosphorus, on the other hand, is an excellent probe since there is a single isotope which has I = 1/2. Vanadium has an isotope with 99.76% natural abundance. Although it has a high spin (I = 9/2) its quadrupole moment is very small so that it serves as an excellent probe of the solid state.

II. KNIGHT SHIFT AND SPIN-LATTICE RELAXATION MEASUREMENTS IN THE PHOSPHIDES WITH THE Ti_3P STRUCTURE TYPE

A. Introduction

In the transition-metal-rich phosphides there are no cases for which compounds in a transition metal group are isostructural, except the group IV and V tri-metal phosphides. At the composition of M_3P (M = transition metal) the Ti_3P structure type exists for six transition metals Ti, Zr, Hf, V, Nb and Ta. This series is ideal for a systematic study of the physical and chemical properties connected with the Ti_3P structure type. Trends in the Knight shift, spin-lattice relaxation and magnetic susceptibility in this series of compounds are utilized to interpret the role of phosphorus in the conduction process. Some qualitative remarks may also be made about the phosphorus binding in these solids.

The Ti_3P structure, shown in Figure 1 taken from the review article by Rundquist (7), can be described as an array of corner and edge sharing tri-capped trigonal prisms. Some of the atoms from Figure 1 have been removed for clarity. Ti_3P crystallizes in the space group $P4_2/n$. There are three structurally inequivalent metal atoms (I, II and III) in this structure but there is one phosphorus atom. The phosphorus atom is located near the center of a trigonal prism at the corners of which are metal atoms. Additional metal atoms are located off each of the three rectangular faces of the

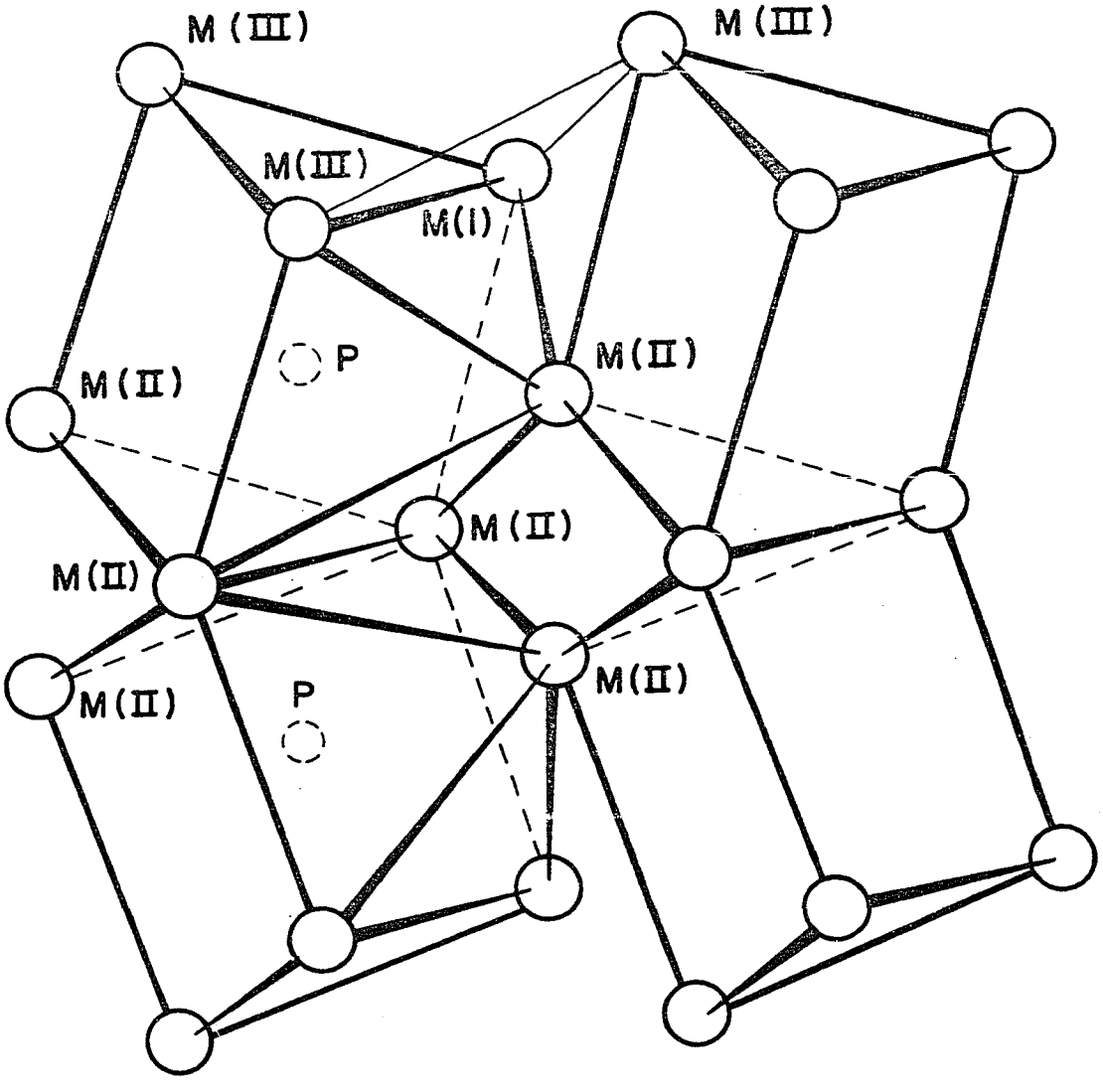

Figure 1. A drawing of the Ti_3P structure. [Some atoms have been removed for clarity. The labels are M for the metal atoms and P for the phosphorus atoms]

trigonal prism, for instance M(I) and M(II). Tri-capped trigonal prismatic coordination for phosphorus, sulfur and other related non-metals is a very common type of coordination.

The monophosphides of most of the first row transition metals and the group III, IV and V transition metals have been studied by NMR. Jones has studied the group IIIb-group Va intermetallics (21) and MnP and $Co_yMn_{1-y}P$ (22). In MnP the phosphorus Knight shift was found to be temperature dependent due to Curie-Weiss behavior of the localized spin at the manganese site. The localized spin on manganese causes a spin polarization of the conduction electrons. Thus the temperature dependence of the phosphorus shift indicates that there are wave functions centered at the phosphorus site which contribute to the make-up of the states at the Fermi surface. In the Curie-Weiss region the Knight shift is, in fact, negative indicating a large contribution from the core polarization term in the total Knight shift. From the studies of the $Co_yMn_{1-y}P$ system Jones (22) observed that the phosphorus shift seemed to be dependent upon the number of d electrons in the conduction band. By use of a K(T) vs χ(T) plot (χ is the magnetic susceptibility and T the absolute temperature) the temperature independent part of the phosphorus Knight shift was determined.

Other transition metal monophosphides have been studied

by Stein and Walmsley (23) and Scott *et al.* (24). Scott *et al.* (24) have studied the magnetic susceptibility and NMR of the monophosphides of Ti, Zr, Hf, V, Nb, Ta and Cr. In CrP the phosphorus shift was temperature dependent and negative in the Curie-Weiss region. The Knight shifts of all of the other phosphides studied by Scott were found to be temperature independent, positive and small. From these studies it was suggested that the phosphorus 3d atomic wave functions can be viewed as making appreciable contributions to the electronic wave functions in the band system.

Although Knight shift data and spin-lattice relaxation times have been used for a number of years to obtain information concerning the contributions of atomic wave functions to the conduction band in metals (25,26,27), no spin-lattice relaxation times were measured for the above mentioned phosphides. In transition metal phosphides which do not have a large local moment, the phosphorus shift is found to be small (between 0.01 and 0.06%). Two interpretations of such data are possible in light of the shift data alone. Small shifts might be diamagnetic (chemical) shifts or small paramagnetic (Knight) shifts. A small Knight shift could arise if $K_s + K_{orb} \cong K_p + K_d$ (see Equation 5). However, the spin-lattice relaxation times are expected to be very different for the two cases.

Knight shift studies together with spin-lattice relaxa-

tion measurements can be expected to yield useful information about the conduction band. For example Narath and co-workers have used Knight shifts along with spin-lattice relaxation times and other data to evaluate the separate contributions to the Knight shift in W (25), Mo (26) and Ir (27).

B. Experimental

All compounds described were prepared in the same manner. Stoichiometric amounts of the elements were mixed in sealed Vycor tubes with residual pressures of $<10^{-5}$ Torr. The purities and suppliers of the starting materials are listed in Table 1. Filing of the metals was done in an inert atmosphere of argon. Iron impurities introduced during filing were removed by use of a strong magnet. The sealed tubes were placed in a low temperature furnace and the temperature raised to between 500 and 700°C, depending upon the sample. After all of the phosphorus had reacted the tubes were removed from the furnace. Sample pellets were formed from the resulting mixture by pressing under vacuum in a tungsten carbide die, followed by isostatic pressing to 50,000 psi. Sealed tungsten crucibles and induction heating were used to anneal the sample pellets to 1500°C in a vacuum of $<10^{-6}$ Torr. In some cases (Ti_3P, Hf_3P and Ta_3P) the high temperature annealing was followed by arc-melting.

Table 1. A listing of the suppliers and purities of the starting materials used in the preparation of the Ti_3P compounds

Element	Supplier	Purity (percent)
Ti	Chicago Development Corp.	>99.95
Zr	Westinghouse-Bettis	99.99
Hf	Pittsburg Naval Reactor	99, ~1% Zr
V	Ames Lab.	>99.99
Nb	Stauffer Metals Corp.	>99.92
Ta	National Research Corp.	99.99
P	Gallard Schlesinger	99.9

The phase identities of the resulting products were determined from Debye-Scherrer X-ray powder photographs and published lattice parameters. A comparison of the intensities and $\sin^2\theta$ values from the powder patterns was made with those either published or calculated using A FORTRAN IV Program for the Intensity Calculation of Powder Patterns (1969 version) by Yvon, Jeitschko and Parthé (28). In the case of Hf_3P an unknown phase persisted after many attempts to eliminate it. This phase represented less than 5% of the total sample. A weak and rather broad NMR line was attributed to this impurity phase. The intensities and diffraction angles from all other samples agreed within experimental error with those calculated.

Two spectrometers were used in the NMR data collection, a standard Varian Associates wide-line spectrometer and a spectrometer designed by D. R. Torgeson (29). Torgeson's spectrometer has a frequency range from 2 to 90 MHz whereas the Varian spectrometer had an upper limit of 16 MHz. Knight shift data were collected using the method of continuous averaging. A 400 channel analyzer was used to store the absorption derivative data from repetitive scans, and thus increase the signal-to-noise ratio. Frequencies up to 26 MHz were used during data collection. Spin-lattice relaxation times were measured using the method of tone-burst Modulation (30) and an apparatus designed by Torgeson and Smith (31). For low temperature experiments the samples were either immersed in liquid nitrogen or cold gas from liquid nitrogen or liquid helium was passed over the sample. The latter method was used to attain temperatures down to 20°K for low temperature Knight shift studies.

Phosphorus Knight shifts were determined using ^{31}P in H_3PO_4 as a reference, or by using ^{7}Li in LiCl solution and the ratio $\nu(P)/\nu(Li) = 1.0413$. Vanadium Knight shifts were measured with respect to the ^{51}V effective gyromagnetic ratio of 1.11927 MHz/kOe using ^{27}Al in $AlCl_3$ solution as the intermediate reference and the ratio of $\nu(V)/\nu(Al) = 1.0089$.

Temperature dependence of the magnetic susceptibility of all samples except Hf_3P was tested by the Faraday method.

The range of temperature was 77° to 300°K. A liquid nitrogen bath was used at 77°K, an isopentane bath from 113° to 273°K and an ice-water bath at 273°K. Susceptibility data were collected at five magnetic fields. A Honda-Owen plot (a plot of susceptibility versus the inverse field strength) was made to extract the contribution to the susceptibility due to ferromagnetic impurities.

C. Results

1. Magnetic susceptibility

Figure 2 summarizes the results of the magnetic susceptibility measurements in a plot of χ(molar) vs T. A susceptibility measurement was not made for Hf_3P. However, it is estimated that the susceptibility of Hf_3P should not be much different than that of Ta_3P (note Zr_3P and Nb_3P). The susceptibilities are temperature independent or weakly temperature dependent and small, indicating Pauli paramagnetism. In the case of V_3P, and perhaps Nb_3P, most of the temperature dependence at low temperatures is attributed to paramagnetic impurities such as iron phosphides which are known to have large magnetic moments (32,33). Further evidence in support of this conclusion is given by the temperature independent Knight shifts. Matthias *et al.* (34) have described V_3P as normal and nonsuperconducting.

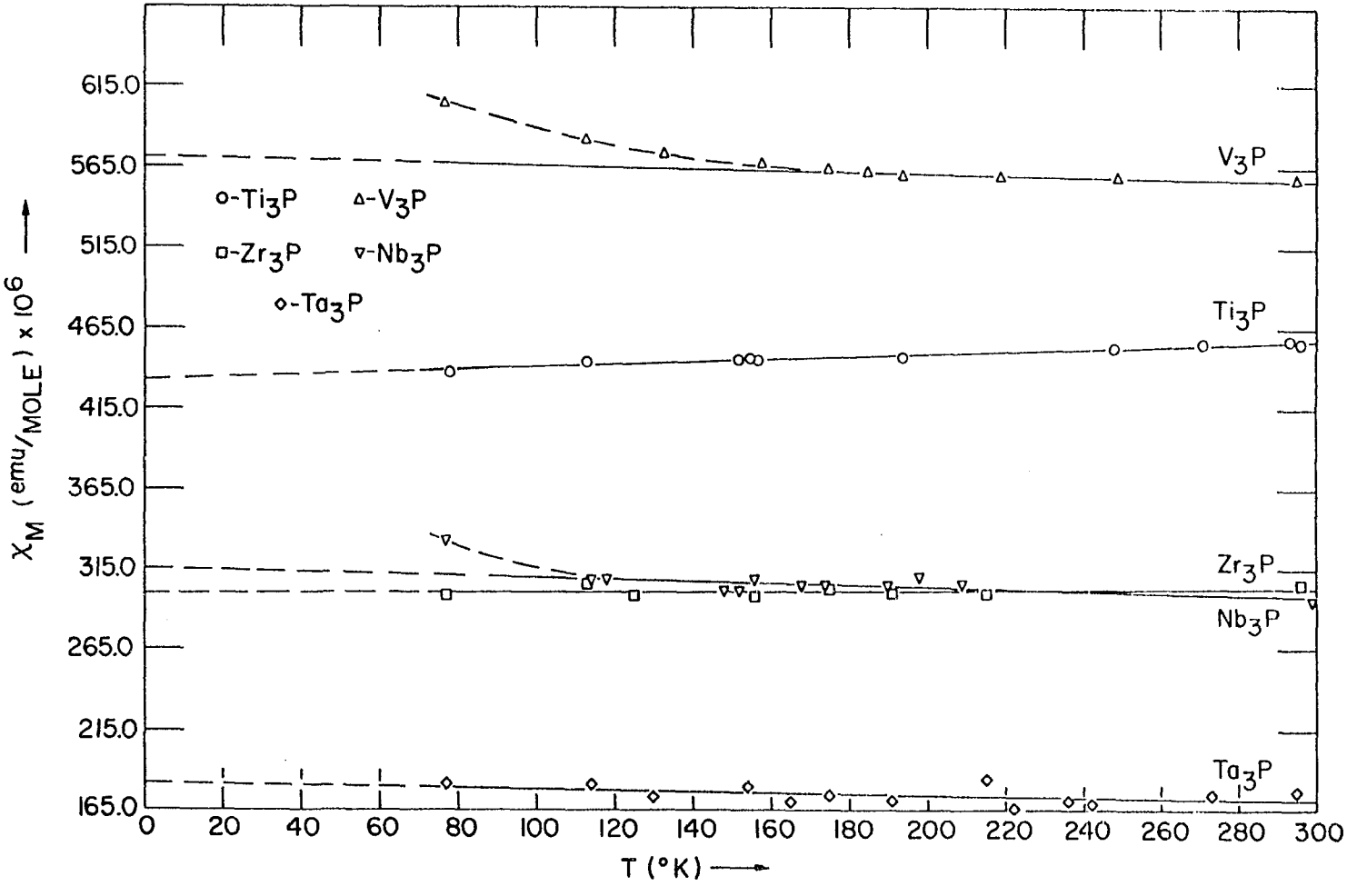

Figure 2. A plot of the molar susceptibility, χ_M, vs the absolute temperature, T

2. Knight shift and spin-lattice relaxation time

In the Ti_3P structure the metal atoms occupy three different sets of 8g positions (the phosphorus atom occupies a fourth set). These positions have point symmetry 1. Both the quadrupole and shift interactions may therefore be expected to exhibit less than axial symmetry.

Summarized in Table 2 are the NMR results. All of the shift values are averages of up-field and down-field scans in order to eliminate any effects of magnet hysteresis. Small positive shifts for ^{31}P were observed, with only the ^{31}P shifts in Zr_3P and Hf_3P showing any measurable anisotropy. No temperature variation of the ^{31}P shifts was observed down to the lowest temperature attained in each instance, i.e., $47^{\circ}K$ (Ti_3P), $85^{\circ}K$ (Zr_3P), $109^{\circ}K$ (Hf_3P), $39^{\circ}K$ (V_3P), $77^{\circ}K$ (Nb_3P) and $103^{\circ}K$ (Ta_3P), at a resonance frequency of 22 MHz.

Although the ^{31}P Knight shifts were small, the spin-lattice relaxation times were short. In Table 2 are listed the values of T_1 at the temperatures $77^{\circ}K$ and $300^{\circ}K$. Experimental problems were encountered in the T_1 determinations. Due to pick-up of the modulation signal, especially at large sweep widths, the base line from which the peak heights are measured became uncertain, so that within the limits of the method used the samples examined have constant values of T_1T.

Knight shifts comparable to the metallic values were found for ^{51}V in V_3P and for ^{93}Nb in Nb_3P, and in the case of

Table 2. Summary of NMR results

Compound[a]	K_{iso}(%)	K_{aniso}(%)	δH(Oe)[b]	T_1(sec, 77°K)	T_1(sec, 300°K)
Ti_3P	0.012(3)[c]	--	2.00(5)	0.62(5)	0.11(5)
Zr_3P	0.023(2)	-0.0064(1)	--	0.38(3)	0.13(6)
Hf_3P	0.030(1)	-0.0070(1)	--	0.57(3)	0.12(4)
V_3P	0.010(4)	--	9.1(2)	0.41(3)	0.11(1)
$^{51}V_3P$(a)	0.59(5)[d] 0.34(5)	--	--	--	--
Nb_3P	0.025(3)	--	8.4(1)	0.27(4)	0.09(3)
$^{93}Nb_3P$	0.9(1)[d]	--	--	--	--
Ta_3P	0.030(3)	--	4.5(1)	0.63(5)	0.15(1)

[a] ^{31}P nucleus unless otherwise noted.

[b] δH is the peak-to-peak width of the absorption derivative.

[c] Figure in parenthesis indicates uncertainty of the last place indicated.

[d] Estimated uncertainty.

V_3P the ^{51}V shift did not vary down to 58°K. The ^{51}V spectrum in V_3P is rather complex and is shown in Figure 3. The central region of this spectrum can be described as resulting from the overlap of two resonances having an intensity ratio of 2:1 and a separation of approximately 40 Oe at 26 MHz. An intensity ratio of 2:1 probably results from two of the sites (M(I) and M(II)) having very similar shifts but different from the third site (M(III)). The Knight shifts obtained in this manner are K = +0.59% for two of the sites and K = +0.34% for the remaining site.

A large number of quadrupole satellite lines were also detected, as evident in Figure 3. No serious attempt was made to assign these lines, due to the complexities introduced by the non-axially symmetric nature of the quadrupole interactions and by the presence of inequivalent sites. For the same reasons, no attempt was made to measure the ^{51}V spin-lattice relaxation time or the shift anisotropy.

Similarly, in the case of the ^{93}Nb resonance in Nb_3P the complex split central transition pattern due to the three inequivalent sites was never resolved. The stated Knight shift (Table 2) was an average value for this spectrum. No attempt was made to determine T_1 in this case.

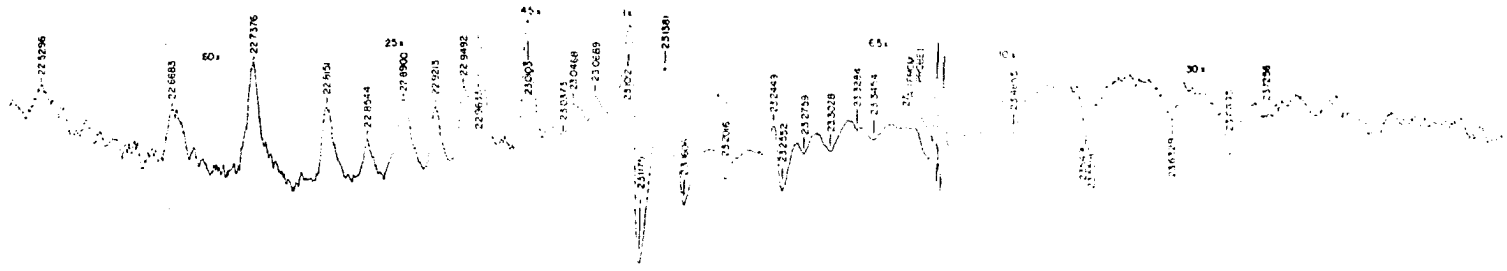

Figure 3. The ^{51}V spectrum in V_3P. [The vertical (intensity) axis has magnifications relative to the central transition (1X) region listed above each section. This scan is up field (horizontal axis).]

D. Conclusions

The magnetic susceptibility data are indicative of the metallic nature of these phosphides. In all cases, the susceptibilities behave very similarly to those of the metals themselves. No anomalies in the temperature dependence are observed, and it seems likely that the departure from straight-line behavior at lower temperatures for V_3P and Nb_3P is due to impurities. Table 3 presents a comparison of the susceptibilities (per gram-atom) with those of the metals (35,36). For more direct comparison, the phosphide values are also given on a per metal atom basis. On this basis the susceptibilities compare very closely in the cases of Ti and Zr, but the phosphide value falls below the metal value in the cases of V, Nb, and Ta by roughly the same magnitude in each case. The signs of the temperature dependence of χ are always the same in the phosphide and in the metal, showing the same (+) and (-) alternation as do the metals, and the magnitudes of the temperature dependences do not differ appreciably. In general terms this comparison indicates that for Ti_3P and Zr_3P the orbital and d-spin contributions to the susceptibility are essentially unchanged from those of the metals. On the other hand, in the cases of V_3P, Nb_3P and Ta_3P, there appears to be a significant reduction in the values of the orbital contribution, χ_{orb}, and/or d-spin contribution relative to those in the metals.

Table 3. Comparison of paramagnetic (molar) susceptibilities of the Ti_3P phosphides and the transition metals. [Units of χ_M are 10^{-6} emu/g-atom, and those of the temperature dependence, $\chi^{-1}(d\chi/dT)$, are 10^{-4} $(^oK)^{-1}$. Data for the metals are from references (35) and (36). (Diamagnetic corrections have not been included)]

	Ti	Ti_3P	V	V_3P	Zr	Zr_3P	Nb	Nb_3P	Ta	Ta_3P
χ_M(at 300°K)	147	457	298	554	120	302	204	296	154	174
χ_M(per metal atom) (at 300°K)	--	152	--	185	--	101	--	99	--	58
$\chi^{-1}(d\chi/dT)$	+1.9	+1.9	-0.6	-0.9	+2.1	+0.6	-0.9	-1.9	-0.7	-2.0

On the basis of the susceptibilities, comparing the case of V_3P with that of vanadium metal, the actual change anticipated in the ^{51}V Knight shift in V_3P is $\Delta K = +0.008\%$ between $77^{\circ}K$ and $300^{\circ}K$. Experimentally, we find that both the ^{31}P and ^{51}V shifts are constant within this temperature range, within the rather large limits of accuracy imposed by the complexity of the V_3P spectrum.

On the other hand, the ^{51}V Knight shift values in V_3P are essentially the same as that in vanadium metal, (see Table 2). This indicates that either the d-spin and orbital contributions to the susceptibility are reduced proportionately so that the net contribution to the Knight shift remains constant, or that the effective hyperfine fields in the phosphides are sufficiently different from those in the metal that the final result again matches that found in the metal.

Phosphorus NMR shifts can be classified into two types. The first type is the relatively small chemical shift which arises from the diamagnetic interaction of the nucleus with the electrons in a completed valence shell. The second type of shift can be large, as in MnP (22), or small, as observed here. In MnP the large temperature dependent phosphorus shift is due to the interaction of the phosphorus nucleus with the spin polarized conduction electrons. Spin polarization of conduction electrons comes about through conduction electron interaction with the local moment on manganese. In MnP the

observed phosphorus Knight shift demonstrates that wave functions centered on the phosphorus nucleus contribute to the conduction band in this metallic compound.

A small NMR shift, as observed here for the Ti_3P-type compounds, might be interpreted as an indication that phosphorus in these phosphides is present with a completed valence shell (i.e., the shift is a chemical shift). However a small paramagnetic shift is expected due to the small hyperfine field of phosphorus (22,37), and similarities in structural and physical properties (excepting the local moment) of MnP and the Ti_3P compounds suggest that the interpretation that the shift is a small Knight shift is more reasonable.

When Knight shifts are small the interpretation is facilitated by spin-lattice relaxation time (T_1) data. For phosphorus with fully satisfied valences, T_1's are expected to be on the order of tens of seconds (e.g., $P_4O_6(\ell, 294^{\circ}K)$, T_1 = 17 sec; P_4O_6(s, 294 K), T_1 = 40 sec (38); P(white, α), T_1 = 28.7 sec (39)) with no proportionality to $(T)^{-1}$. For nuclei in metals on which conduction electrons have some finite probability density T_1's are expected to be substantially shorter.

In the Ti_3P compounds T_1's are in the 0.1 sec range. These T_1's are consistent with substantial coupling of the phosphorus nuclei to the lattice via conduction electrons. Thus the phosphorus relaxation times show that the phosphorus NMR shift is a Knight shift, and that phosphorus wave func-

tions are included in the states which appear at the Fermi surface.

Although an evaluation of the various components of the total Knight shift shown in Equation 5 must await other experimental data, such as low temperature heat capacities, and calculations, such as a good tight-binding band calculation, trends are observed which may give indications at least of the important contributions. The similarities between the susceptibilities of the pure metals and the Ti_3P compounds has been noted above. The observed decrease in susceptibility in the elemental metals has been attributed to a decreasing density of states toward the heavier elements in a group (40). Increasing metal Knight shifts are observed for the same direction within a group. It has been shown that the increase in Knight shift with decreasing susceptibility is generally due to the relative increase in the orbital Knight shift (25, 26,41,42). In the Ti_3P compounds the phosphorus Knight shift similarly increases with decreasing susceptibility. It might therefore be expected that the same relative contributions to K_{tot} from its components are found for phosphorus in Ti_3P compounds. Support for this conclusion is found in the T_1 results. Table 4 compares values of T_1T observed for phosphorus in Ti_3P compounds with the values calculated using the Korringa relation (43),

$$T_1T = \frac{\Delta\mu_B^2}{\pi k\hbar\gamma^2K^2} \qquad (13)$$

assuming that the shift arises solely from the contact interaction and $\Delta = 1$. A measure of how well experiment agrees with the contact only theory is given by Δ. In the first transition row Ti_3P compounds the calculated T_1T is much greater than the observed value, whereas the situation is reversed for the Ti_3P compounds of the second and third row. If the observed increase in K_{tot} is due to a relative increase in importance of K_s, then a better fit to Equation 13 would be expected. Thus it is concluded that the observed trends in Knight shift, magnetic susceptibility and spin-lattice relaxation times are suggestive of importance of the orbital and core-polarization contributions to the phosphorus Knight shift. These contributions, together with the metallic nature of these solids, suggest that the phosphorus wave functions contributing to binding and conduction contain configurations higher in energy than the ground state.

Table 4. A comparison of the values of T_1T observed and calculated using Equation 13

Compound	T_1T (sec-deg Kelvin) Observed	Calculated
Ti_3P	33.9	70.3
Zr_3P	33.0	19.1
Hf_3P	35.4	11.2
V_3P	32.4	101.2
Nb_3P	27.6	16.2
Hf_3P	44.4	11.2

III. KNIGHT SHIFT MEASUREMENTS IN THE $VS_{1\pm x}$ SYSTEM

A. Introduction

Early structural studies by Biltz and Köcher (3) and Hoschek and Klemm (44) provided evidence that the NiAs structure type exists for vanadium monosulfide on the sulfur rich side of stoichiometry. Pedersen and Grønvold (45) confirmed these observations. Tsubokawa (46) observed a transition at 1040°K in the magnetic susceptibility and specific heat of a sample of VS (of unspecified composition). He considered this transition to be a Néel or antiferromagnetic ordering. Four years later Franzen and Westman (47) reported that in the portion of the VS_{1-x} homogeneity region for which $0.85 \leq S/V \leq 1.05$ the monosulfide has the MnP structure type and they suggested the existence of, at most, an unusually narrow VS_{1-x}-VS two phase region. Later Franzen and Burger (48) reported that there was no two phase region and that the homogeneity range of VS extended from $VS_{0.92}$ to $VS_{1.17}$. It was reported that from $VS_{0.92}$ to $VS_{1.064}$ the MnP structure type is stable and from $VS_{1.064}$ to $VS_{1.17}$ the NiAs structure type is stable. The absence of a two phase region implies that the volume and the entropy change continuously and thus that a second order phase transition occurs with increasing sulfur concentration. That the volume changes continuously is evident from Figure 4. It was also shown that in metal rich VS there are sulfur vacan-

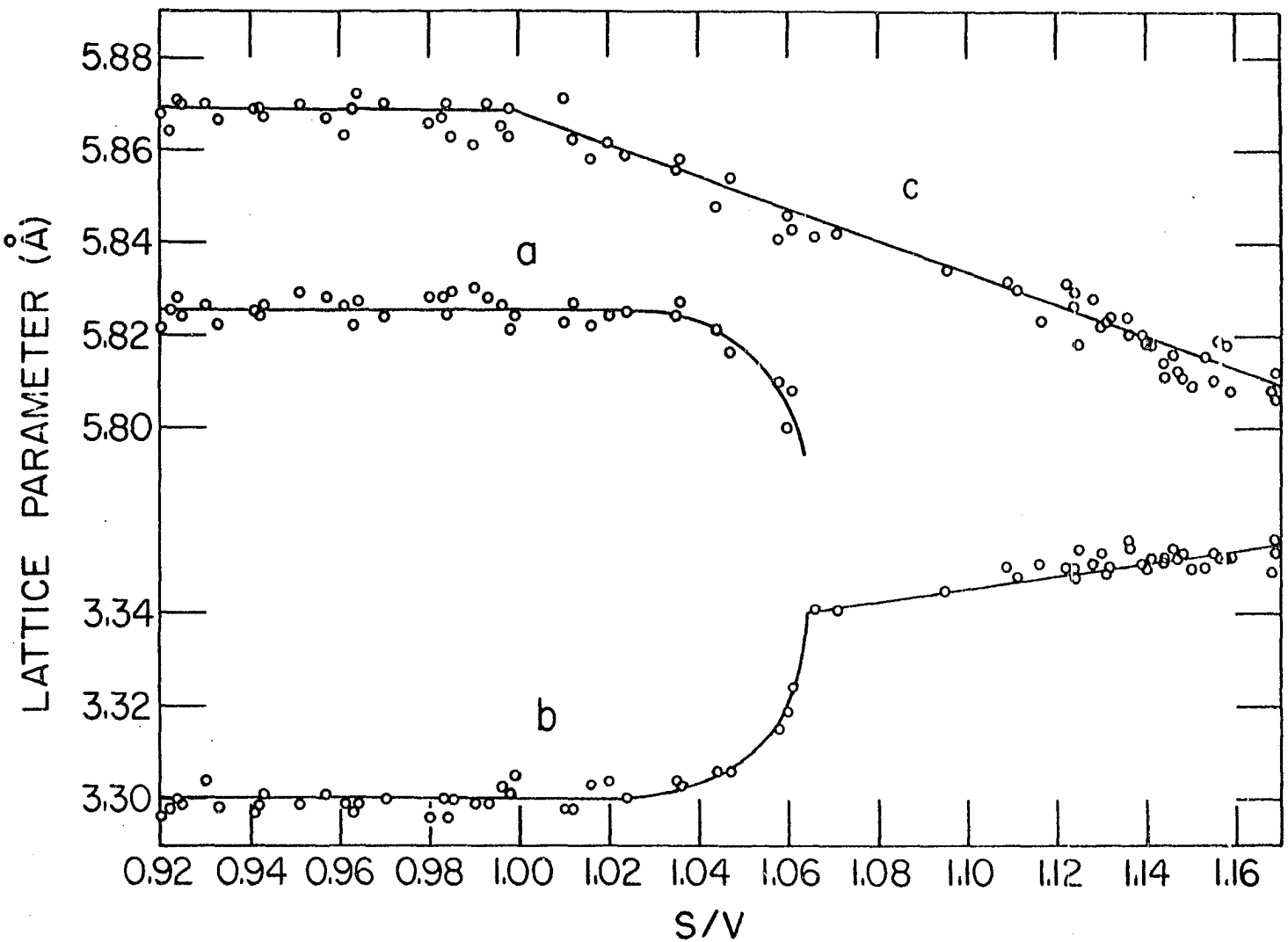

Figure 4. A plot of the lattice parameters (Å) vs the sulfur to vanadium ratio (S/V). [The parameters are labeled in accordance with the space groups P_{cmm} and $P6_3/mmc$ so that the orthorhombic c and b axes transform into the hexagonal c and a axes, respectively]

cies and in the sulfur rich VS there are vanadium vacancies.

The research reported here was initiated to determine if either of the compounds in the VS system are antiferromagnetic, to determine what effect vacancies of different types (i.e. sulfur and vanadium) have upon the ^{51}V NMR resonance, and to determine the effect of the structure change upon the ^{51}V NMR resonance. Barnes and Creel (49) observed the extinction of the ^{11}B resonance at the Neel temperature in CrB_2, suggesting that in compounds with antiferromagnetic ordering the NMR signal is not readily observed, presumably due to the very large local field. The study of the effect of vacancies on the ^{51}V resonance was unsuccessful. However, the change in the Knight shift with increasing S/V ratio yields rather useful information concerning the conduction electrons, and hence the conduction band in the neighborhood of the Fermi energy, as the S/V ratio is varied, especially through the transition point in the monosulfide.

B. Experimental

Samples of VS were prepared in the same manner as described for the phosphides. An intermediate step was added to the preparative procedure which greatly reduced the loss of sulfur during high temperature annealing and made the control of stoichiometry more tractable. After the 1/2" x 1" sample pellet was formed it was transferred to an outgassed,

3/4" x 2" tantalum tube one end of which had been capped and sealed by electron-beam welding. This transfer took place inside an argon-filled dry box. A lid was force-fit into the other end of the tube and this assembly placed in the electron-beam welder which was then pumped down to $<10^{-5}$ Torr. The sealed tantalum tube was placed in an evacuated Vycor tube which was closed via a stopcock. The sample was placed in a furnace maintained at about 850°C for four to seven days. Removal of the sample from the tantalum tube, followed by induction heating at 1350° to 1400°C in a sealed tungsten crucible, completed the sample preparation.

Structure type and lattice parameters of the resulting samples were determined by Debye-Scherrer and Guinier X-ray powder photographs. Lattice parameters were obtained by the method of least squares refinement of the observed 2θ values. These lattice parameters along with the plot of lattice parameters versus sulfur to vanadium ratio, Figure 4 from Franzen and Burger (48), were used to determine the stoichiometry of each sample. Table 5 lists the sample and stoichiometry. Starting material purities were for vanadium and sulfur >99.99% and 99.999%, respectively.

NMR data were collected in the same manner as described earlier. Low temperature measurements were made at 77°K using liquid nitrogen.

Table 5. A listing of the sulfur to vanadium ratios for the ten VS samples

Sample	Structure type	Stoichiometry (S/V)[a]
VS-7	MnP	0.966
VS-3	MnP	1.007
VS-5	MnP	1.010
VS-9	MnP	1.039
VS-8	MnP	1.041
VS-10	MnP	1.058
VS-6	NiAs	1.106
VS-4	NiAs	1.129
VS-2	NiAs	1.135
VS-1	NiAs	1.142

[a]Estimated uncertainty in the S/V ratio is <0.010.

C. Results

Table 6 lists the NMR results for the ten samples prepared in the order of increasing sulfur content (see Table 5). Spectra were taken at operating frequencies of 4.5, 13, 20 and 26 MHz. In all samples the line width (peak-to-peak absorption derivative) was linear with the applied field, as shown for three samples in Figure 5. Typical resonance line shapes are reproduced in Figures 6 and 7 for the operating frequencies of 4.5 and 13 MHz to illustrate the broadening of the line with increasing sulfur or vanadium vacancy concentration. Although the spectra for samples more sulfur rich than $VS_{1.058}$ display evidence of an anisotropic shift, the anisotropic shift peak is sufficiently broad as to be unmeasurable.

Table 6. A summary of the NMR data for the VS_{1+x} system. [The samples listed in order of increasing composition as in Table 5]

Sample	% shift @ (MHz) 300°K				δH^a (Oe) @ (MHz)				% shift @ 77°K (MHz)
	4.5	13	20	26	4.5	13	20	26	4.5
7	0.179[b]	0.192	--	0.184	10.0[c]	20.2	--	39.6	0.188
3	0.178	0.192	0.188	0.192	9.2	21.2	27.4	37.4	0.196
5	0.176	0.189	0.192	0.189	10.0	21.1	27.4	38.4	0.189
9	0.187	0.224	--	0.206	10.6	24.5	--	40.8	0.223
8	0.181	0.190	--	0.183	9.7	21.0	--	40.0	0.210
10	0.245	--	0.250	--	--	--	35.2	--	0.231
6	0.252	0.298	--	0.312	13.6	27.6	--	48.7	0.238
4	0.261	0.282	--	0.305	13.2	28.6	--	46.8	0.294
2	0.238	0.268	0.260	0.269	13.1	28.0	41.9	53.1	0.266
1	0.261	0.304	--	0.325	14.5	29.2	--	53.4	0.303

[a]Peak-to-peak absorption derivative line width.

[b]Estimated uncertainty in the Knight shift is 0.005%.

[c]Estimated uncertainty in the peak width is 0.5 Oe.

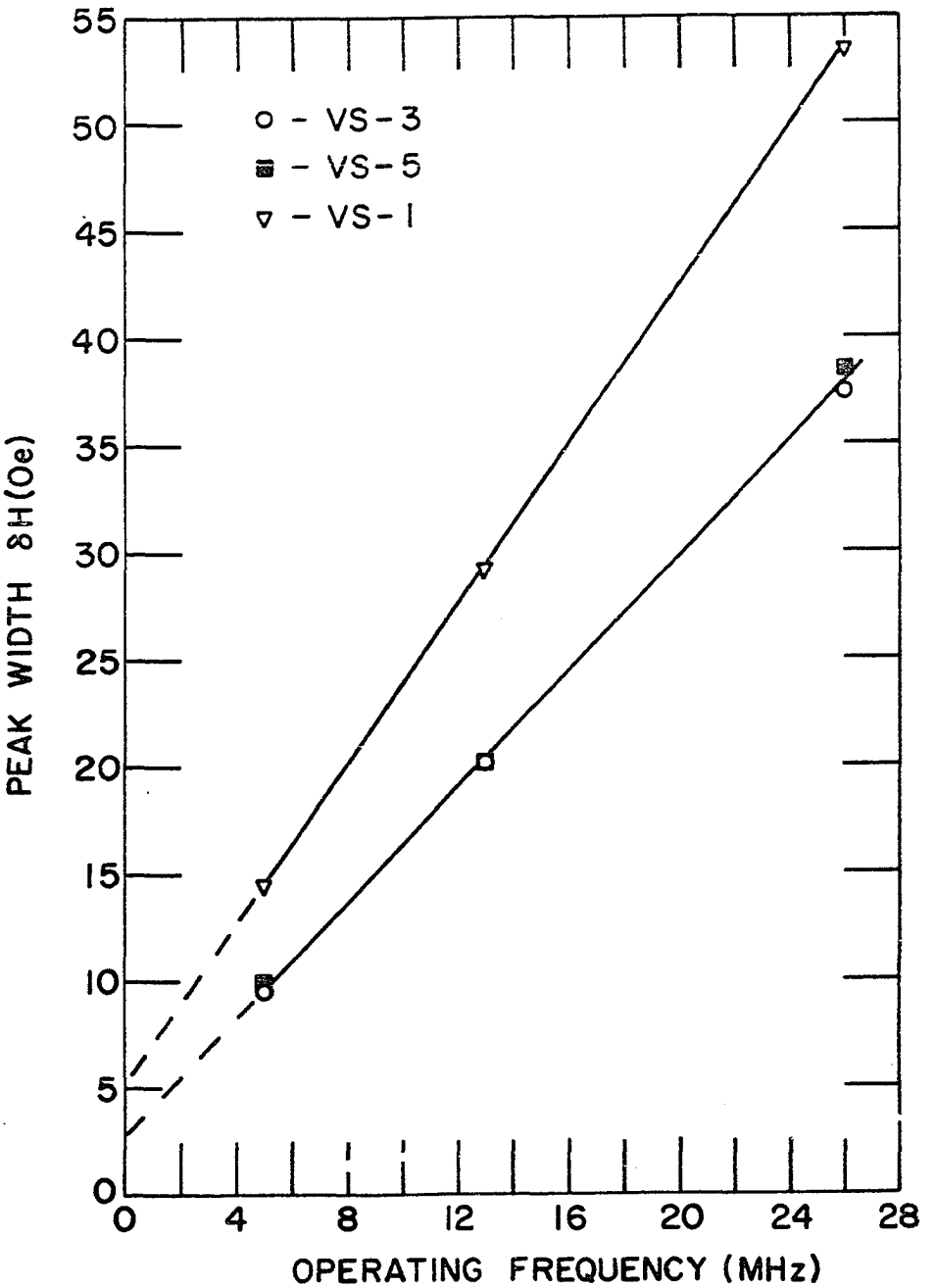

Figure 5. A plot of peak width (Oe, peak-to-peak absorption derivative) vs operating frequency (MHz) for three representative samples in the $VS_{1\pm x}$ system

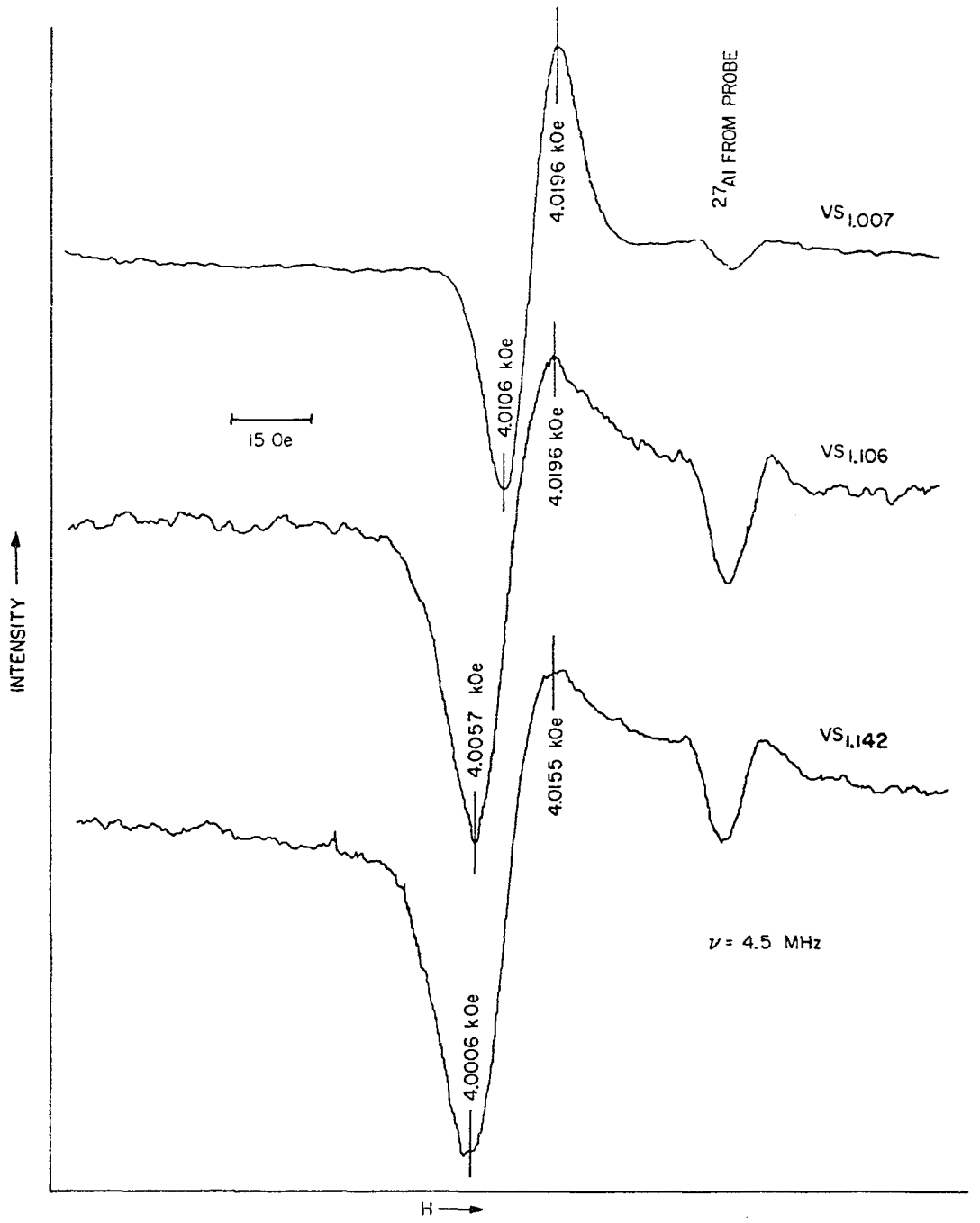

Figure 6. Traces of the derivative spectrum for three representative samples at an operating frequency of 4.5 MHz

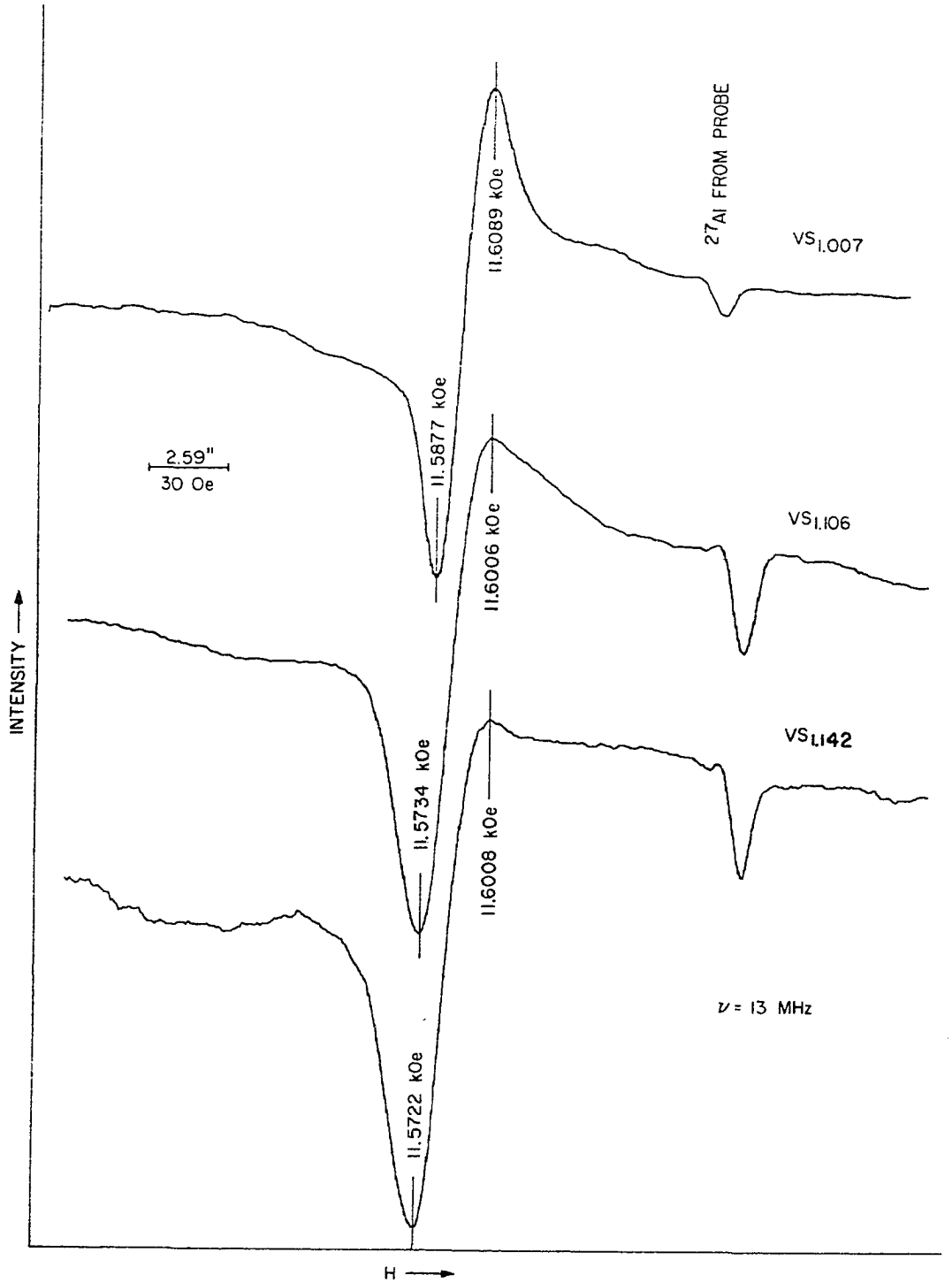

Figure 7. Traces of the derivative spectrum for three representative samples at an operating frequency of 13 MHz

For this reason the most accurate value of the shift was selected from the 4.5 MHz spectra and this shift value is plotted against the S/V ratio in Figure 8. Interference from the aluminum resonance arising from the probe becomes sizeable at lower frequencies. The observed shifts for samples more sulfur rich than $VS_{1.058}$ were field dependent.

Only a small temperature dependence of the Knight shift was observed (see Table 6). Increases of about 0.01 to 0.04% in the Knight shift were observed. No decrease in the intensity of the resonances was observed.

In the samples with composition $VS_{0.966}$ to $VS_{1.058}$ (i.e. the samples within the MnP structure range) the resonance line was more symmetrical than those observed for the compositions $VS_{1.106}$ and greater. Although the peak-to-peak width of the absorption derivative is field dependent, there is no evidence for an anisotropic shift. In the compounds with symmetric lines some resolution of the quadrupole spectrum was observed. However, sufficient resolution was not obtained to identify the transitions. These quadrupole transitions occurred as shoulders on the absorption derivative peak. A rough calculation showed that there should be no significant contribution to second order quadrupole splitting of the central transition.

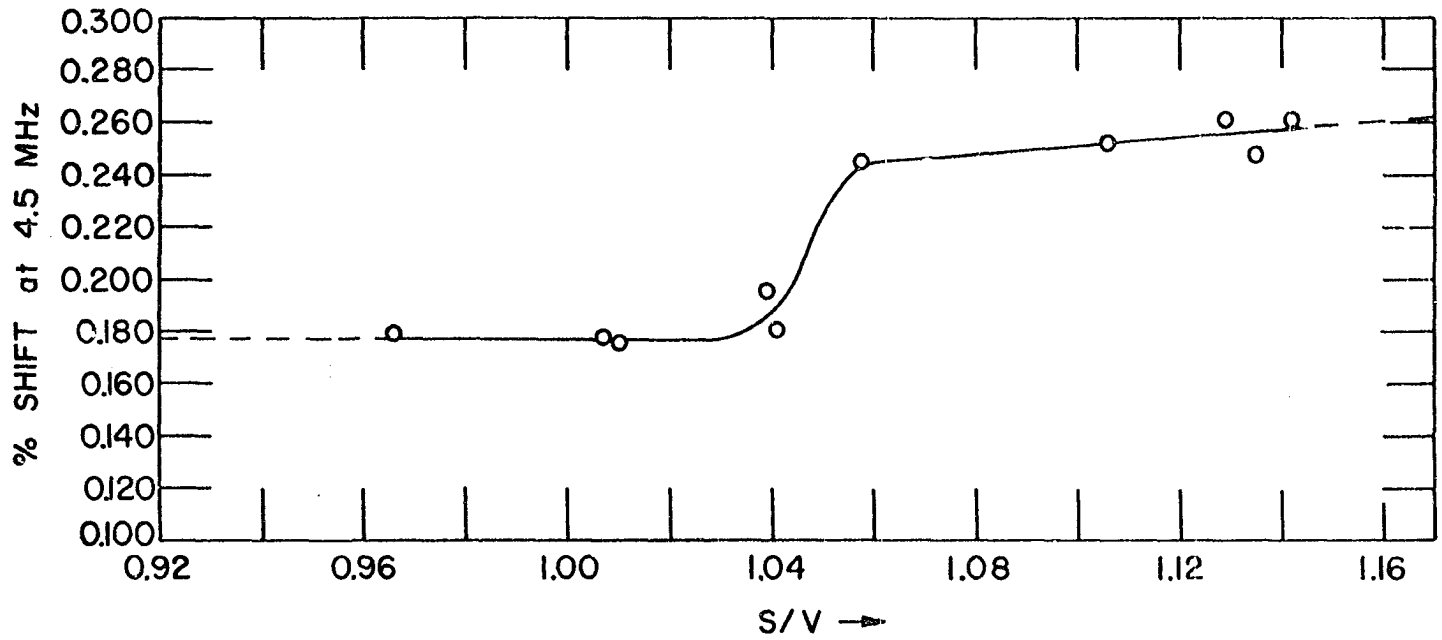

Figure 8. A plot of the Knight shift (%) vs the sulfur to vanadium ratio (S/V)

D. Conclusions

On the basis of the strength of the ^{51}V NMR signal it is concluded that these compounds are not antiferromagnetic as was suggested by Tsubokawa (46). This conclusion suggests that the transitions observed by Tsubokawa (46) may be structural.

A computer synthesis of an anisotropically broadened line was performed using a constant K_{ax} but several values of K_{iso}. This was accomplished by integrating

$$G(X) = A\left(1 + \frac{2}{\Delta\nu_{\parallel}}\right)^{-\frac{1}{2}}\left(\frac{2}{\sqrt{\pi}\sigma}\exp\left(-\frac{4(X-X_o)^2}{\sigma^2}\right)\right), \qquad (13)$$

where A is the amplitude of the absorption peak, the second term is obtained from the variation of the frequency shift with $\cos\theta$ about K_{iso} and the last term is the gaussian distribution function with 0.5σ as the half-width of the gaussian peak. Figure 9 shows three such plots of the absorption derivative for different values of σ and E(K). The factor E(K) was used to shift the value of K_{iso} by an amount (0.005) E(K). For instance K_{iso} would be shifted in arbitrary units by 0.05 for E(K) equal to 10 or -0.05 for E(K) equal to -10. Five values of E(K) were used in each case, two positive, two negative and zero. In all cases the relative intensity ratio of the peaks was 0.25:0.50:1:1:0.50:0.25. Increasing E(K) has the same effect as increasing the magnetic field. As E(K)

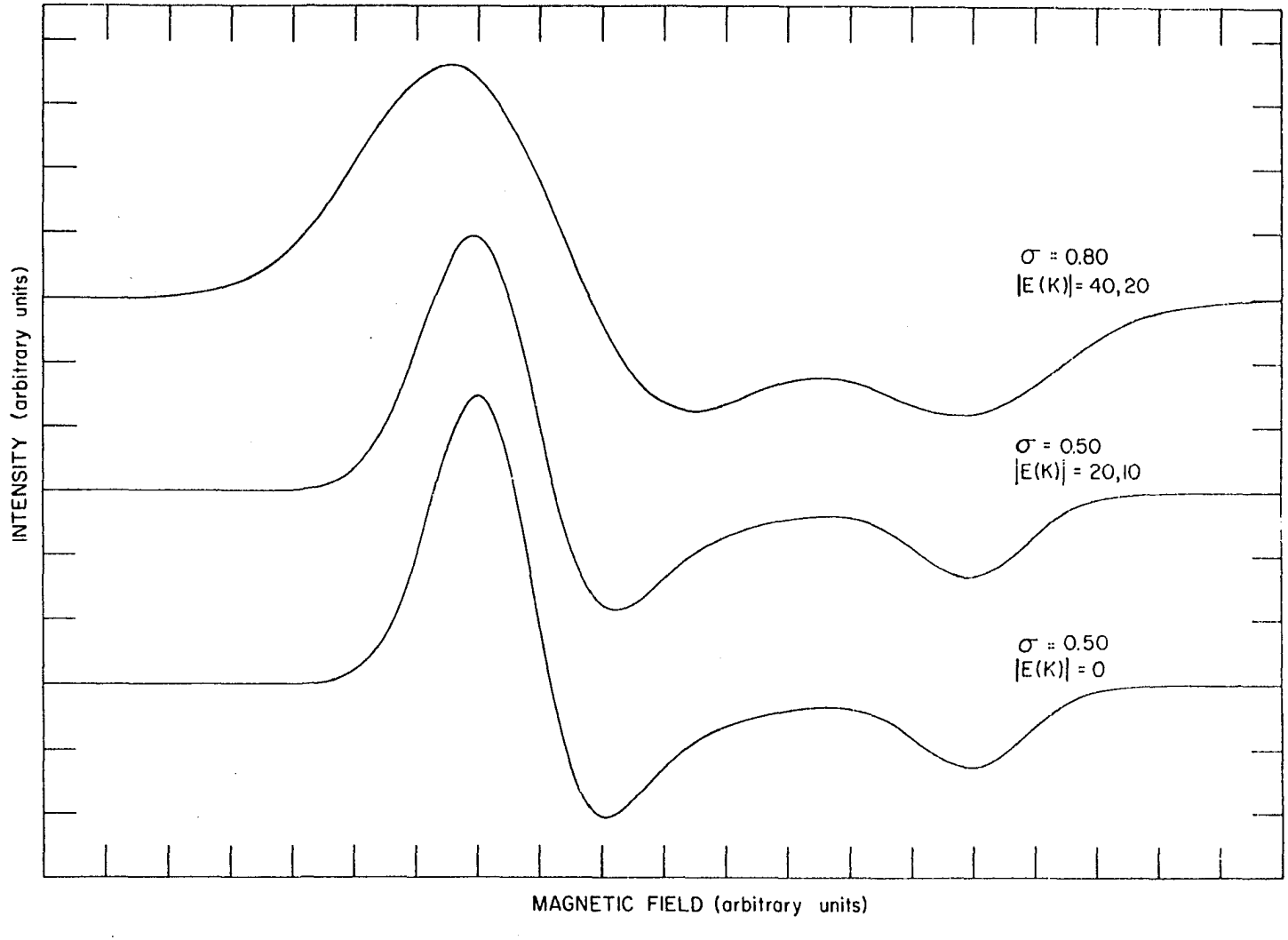

Figure 9. Three computer synthesized line shapes demonstrating the effect on line shape of a distribution of K_{iso} values

becomes larger the line becomes broader, which is what is observed for the lines reported here. However, a broadening of the peak with increasing magnetic field may also occur for the case of less than axial symmetry where three unequal shift values might occur. Less than axial symmetry is to be expected due to the introduction of vacancies into the solid. A differentiation between these two possibilities may be possible upon the availability of a superconducting magnet in which an operating frequency of 65 MHz may be possible. At that frequency it may also not be possible to distinguish between the two cases since the observed anisotropic peak is rather broad and another peak due to non-axial symmetry might be expected to be equally broad. In any case it must certainly be the case that K_{ax} has some distribution of values as well as K_{iso}, since the K_{ax} peak is unresolved in compounds with greater sulfur content than $VS_{1.058}$.

Field dependence of the Knight shift where an anisotropic shift is observed is certainly expected since the measured peak actually corresponds to $K_{\perp}$ and not K_{iso}. The values for the shift reported in Table 6 at 4.5 MH and plotted in Figure 8 are probably not more than 5 to 8% in error since $VS_{1.058}$ (K = 0.245%) has no observed axial peak and has a field independent Knight shift.

Figures 4 and 8 have marked similarities in that the b lattice parameter and the Knight shift increase together from

$VS_{1.02}$ to $VS_{1.064}$ in the MnP structure range and from $VS_{1.064}$ in the NiAs structure range. A decrease in the vanadium concentration with a concomitant increase in the vanadium Knight shift is consistent with the removal of d electrons from the conduction band. A decrease in the d states and electrons in the conduction band (i.e. in a rigid band model) is expected to increase the relative importance of the positive terms in Equation 5, K_s and/or K_{orb}. Consider the removal of d electrons from a rigid band. In this case K should increase since K_d would be decreasing in magnitude corresponding to fewer electrons with non-s wave functions.

The observed trend in crystal structure of the first row transition metal monophosphides and monosulfides is consistent with the above interpretation. The stoichiometric compounds VS and CrP crystallize with the MnP structure type, whereas VP and TiS crystallize with the NiAs structure type. Removal of one valence electron per formula unit from VS corresponds to either VP or TiS. The same number of valence electrons as in VS is represented by CrP. A change of symmetry by withdrawal of conduction electrons without apparent loss of metallic character or change in magnetic character indicates the overlap of two conduction bands in the rigid band model; one with symmetry consistent with the MnP structure type and one with the NiAs structure type. The top of the NiAs symmetry band would lie lower than that of the MnP

band. From the above trend it can be said that in the rigid band model eight electrons per formula unit stabilize the NiAs structure, whereas nine electrons per formula unit stabilize the MnP structure. This trend fits the observed structural transition in the VS system which occurs at 8.4 electrons per formula unit obtained by calculating the electron concentration. Correlated with this trend is the observed ^{51}V Knight shift in VP which is +0.303% (25), in fair agreement with the shift reported here for VS with the NiAs structure type.

For the first row transition metal monophosphides from CrP to CoP the MnP structure is maintained but the magnetic properties change from Pauli paramagnetic to ferromagnetic and back to Pauli paramagnetic. Seemingly the best explanation of this change in magnetic properties (see Pauling (18) pp 393-404) is that the extra electrons added (above the nine required for the MnP structure type) go to fill non-bonding orbitals. This interpretation is consistent with the observed and calculated contraction of the transition metal d orbitals in the first row.

Trends observed for the ^{51}V Knight shift in the VS system and structures of VS, VP, TiS and CrP are consistent with the interpretation that the removal of electrons via removal of vanadium atoms from VS lowers the Fermi energy to a point within the conduction band at which the NiAs structure type is stable with respect to the MnP structure type.

IV. PROPOSALS FOR FURTHER WORK

Phosphorus should be utilized more often in the study of the solid state NMR. Having a 100% isotopic abundance and spin I = 1/2 make it ideally suited as a probe of many high temperature compounds. Other than the obvious suggestion of studying other metal-phosphorus systems there is the possibility of studying ternary systems of metal, sulfur and phosphorus. An extension of the VS work presented here would be the study of the ternary (or pseudo binary) systems VP-VS, TiS-VP and VS-CrP. Also the VS-TiS system could be studied using the ^{51}V nucleus as a probe. These systems should provide ample data for the definition of the conduction band in the MnP and NiAs structure types and a better understanding of the MnP to NiAs structural transition which occurs for a number of 1:1 compounds.

Simple systems should be sought in which the nuclei ^{77}Se and ^{125}Te could be used. These nuclei have spin I = 1/2 but low isotopic abundances (ca. 7%).

Tsubokawa (46) reported that VSe has a Néel temperature of 163°K. NMR can be used as in VS to determine if the observed transition is due to magnetic ordering or a structural transformation. It appears from the VS results reported above that the MnP structure type is the low temperature structure type. The structure reported for VSe is NiAs (6).

To further confirm the NMR results high temperature X-ray studies should be made on VS, and low temperature X-ray studies should be made on VSe.

V. BIBLIOGRAPHY

1. Drain, L. E., Metallurgical Rev., 12 (119), 195 (1967).

2. Biltz, W., Ehrlich, P. and Meisel, K., Z. Anorg. Allg. Chem., 234, 97 (1937).

3. Biltz, W. and Köcher, A., Z. Anorg. Allg. Chem., 241, 324 (1939).

4. Jellinek, F., Arkiv for Kemi, 20, 447 (1963).

5. Haraldsen, H., Angew. Chem., Internat. Edit., 5 58 (1966).

6. Hulliger, F., Structure and Bonding, 4, 83 (1968).

7. Rundquist, S., Arkiv for Kemi, 20 (7), 67 (1962).

8. Aronsson, B., Lundström, T., and Rundquist, S., Borides, Silicides and Phosphides - A Critical Review of Their Preparation, Properties and Crystal Structure, John Wiley and Sons Inc., New York, 1965.

9. Aronson, B. and Rundquist, S., Acta Cryst., 15, 878 (1962).

10. Franzen, H. F. and Graham, J., J. Inorg. Nucl. Chem., 28, 377 (1966).

11. Owens, J. P., Conard, B. R. and Franzen, H. F., Acta Cryst., 23, 77 (1967).

12. Franzen, H. F., Beineke, T. A. and Conard, B. R., Acta Cryst., B24, 412 (1968).

13. Conard, B. R., Norrby, L. J. and Franzen, H. F., Acta Cryst., B25, 1729 (1969).

14. Franzen, H. F., J. Inorg. Nucl. Chem., 28, 1575 (1966).

15. Slater, J. C., J. Chem. Phys., 41, 3199 (1964).

16. Rundle, R. E., Acta Cryst., 1, 180 (1948).

17. Rundle, R. E. and Olson, D. H., Inorg. Chem., 3, 596 (1964).

18. Pauling, L., The Nature of the Chemical Bond (3rd ed.) Cornell University Press, New York, 1960.

19. Conard, B. C. and Franzen, H. F., The Chemistry of Extended Defects in Non-Metallic Solids, North-Holland Publishing Co., Amsterdam, Holland, 1970.

20. Franzen, H. F., Department of Chemistry, Iowa State University, Ames, Iowa (private communication, 1970).

21. Jones, E. D., Phys. Rev., 180 (2), 455 (1969).

22. Jones, E. D., Phys. Rev., 158 (2), 295 (1967).

23. Stein, B. F. and Walmsley, R. H., Phys. Rev., 148 (2), 933 (1966).

24. Scott, B. A., Eulenberger, G. R. and Bernheim, R. A., J. Chem. Phys., 48 (1), 263 (1968).

25. Narath, A. and Fromhold, A. T., Jr., Phys. Rev., 139 (3), A794 (1965).

26. Narath, A. and Alderman, D. W., Phys. Rev. 143 (1), 328 (1968).

27. Narath, A., Phys. Rev., 165 (2), 506 (1968).

28. Yvon, K., Jeitschko, W. and Parthé, E., A FORTRAN IV Program for the Intensity Calculation of Powder Patterns (1969 version), School of Metallurgy and Materials Science, University of Pennsylvania, Philadelphia, Pennsylvania, 1969.

29. Torgeson, D. R., Rev. Sci. Instr., 38, 612 (1967).

30. Look, D. C. and Locker, D. R., Phys. Rev. Letters, 20 (18), 987 (1968).

31. Torgeson, D. R. and Smith, W. C., Rev. Sci. Instr., 40, 583 (1969).

32. Cadeville, N. C. and Meyer, A. J. P., Compt. Rend. Acad. Sci. Paris, 252, 1124 (1961).

33. Blaugher, R. D., Hulm, J. K. and Yocum, P. N., J. Phys. Chem. Solids, 26, 2037 (1965).

34. Matthias, B. T., Wood, E. A., Corenzwit, E. and Bala, Y. B., J. Phys. Chem. Solids, 1, 188 (1956).

35. Shimizu, M. and Takahashi, T., J. Phys. Soc. Japan, 15, 2236 (1960).

36. Drain, L. E., Proc. Phys. Soc. (London), 83, 755 (1964).

37. Freeman, A. J. and Watson, R. E., Magnetism, (G. T. Rado and H. Suhl, Eds.), Vol. IIA, Chapt. IV, Academic Press Inc., New York, 1965.

38. Dagfinn, W. A., Acta Chem. Scand., 23, 1078 (1969).

39. Reing, H. A., J. Chem. Phys. 37, 2575 (1962).

40. Gschneidner, K. A., Jr., Physical Properties and Interrelationships of Metallic and Semimetallic Elements. In Seitz, F. and Turnbull, D., eds. Solid State Physics. Vol. 16. Academic Press, Inc., New York, New York, 1965.

41. Shimizu, M., Takahashi, T., and Katsuki, A., J. Phys. Soc. Japan, 18 (8), 1192 (1963).

42. Van Ostenburg, D. O., Lam, D. J., Shimizu, M. and Katsuki, A., J. Phys. Soc. Japan, 18 (12), 1744 (1963).

43. Abragam, A., The Principles of Nuclear Magnetism, Oxford University Press, Oxford, England, 1961.

44. Hoschek, E. and Klemm, W., Z. Anorg. Allgem Chem., 242, 49 (1939).

45. Pedersen, B. and Grønvold, F., Acta Cryst., 12, 1022 (1959).

46. Tsubokawa, I., J. Phys. Soc. Japan, 14 (2), 196 (1959).

47. Franzen, H. F. and Westman, S., Acta Chem. Scand., 17, 2353 (1963).

48. Franzen, H. F. and Burger, T. J., J. Chem. Phys., 49 (5), 2268 (1968).

49. Barnes, R. G. and Creel, R. B., Phys. Letters, 29A, 203 (1969).

VI. ACKNOWLEDGEMENTS

This thesis represents one of the few collaborative efforts on the part of members of the departments of different scientific disciplines. Experiencing different disciplines through course-work leads only to a delusion of an inter-disciplinary experience. However, experiencing another scientific discipline through combined efforts on a research project is second only to joining that discipline.

The author wishes to express his gratitude to Dr. H. F. Franzen and Dr. R. G. Barnes of the Physics Department for the opportunity to take part in this interdisciplinary effort and for their guidance and cooperation throughout the project.

The author wishes also to acknowledge the members of Dr. Barnes' group who helped in the understanding of the instrumentation. Of these members a special mention is made of David Torgeson whose mastery of electronics provided the 2 to 90 MHz spectrometer and other specialized equipment used throughout this project and of Richard Schoenberger for providing the basic computer program for line shape synthesis and assistance in its modification.

Dr. Franzen's group as always provided a relaxed and stimulating atmosphere for both work and recreation, for which the author will always be indebted.

Although foremost, the final acknowledgement is of my

wife, Marietta, whose continual love and understanding provided a most relaxed and enjoyable home during the course of graduate school.

VII. APPENDIX

A. The Method of Tone-Burst Modulation

Tone-burst modulation is a relatively new method for the determination of spin-lattice relaxation times. A brief explanation of the experimental apparatus will be made first (for a complete description see reference (31)), followed by an explanation of the experiment. Use is made of the existing modulation coils in a conventional NMR probe. A conventional spectrometer using the normal detection techniques and associated apparatus is utilized. A triangle wave is passed through the modulation coils and a triangularly varying magnetic field results. Adjustment of the field produced by the spectrometer magnet is made such that the resonance condition for the particular nucleus at the operating frequency is met about half of the way along the side of the triangle wave.

The experiment starts with the triangle wave turned off. One scan contains n passes through resonance where n is twice number of cycles of the triangle wave. The first passage through resonance starts with the spin system in thermal equilibrium with the lattice. Adjustment of the frequency of the triangle wave is made such that the spin system is unable to return to equilibrium between the first and second passage through resonance. Thus, upon passage through resonance the second time, the difference in population of the two Zeeman

levels (assuming spin I = 1/2) has decreased, and the intensity of the second absorption line is less than the first. The intensity of the absorption will continue to decrease until a new equilibrium is established between the spin system and the lattice in the presence of the oscillating field and radio frequency power. This new equilibrium is established after a large number of passes through resonance such that an undetectable difference in the intensity maxima has been achieved. The rate at which this new equilibrium is approached is determined in the first part of the experiment.

The first part of the experiment is illustrated in the top trace of Figure 10. Here 4.5 cycles of the triangle wave were used. At the end of one scan the triangle wave is turned off. The spin system is allowed to return to equilibrium with the lattice, after which another scan is made. Successive scans are stored in a multichannel analyzer to improve the signal to noise ratio. Figure 10 represents the output from the analyzer. To obtain the value of the absorption intensity for the equilibrium at "infinity" the triangle wave is left on all of the time, and the same number of scans are collected in the analyzer. This is the second part of the experiment, and is represented by the lower trace in Figure 10.

To obtain T_1 a plot of $\ln(H_n - M_\infty)$ vs n is made where H_n is is the amplitude of the nth peak and M_∞ is the amplitude of the "infinite" peak. Using the slope, S, and the intercept,

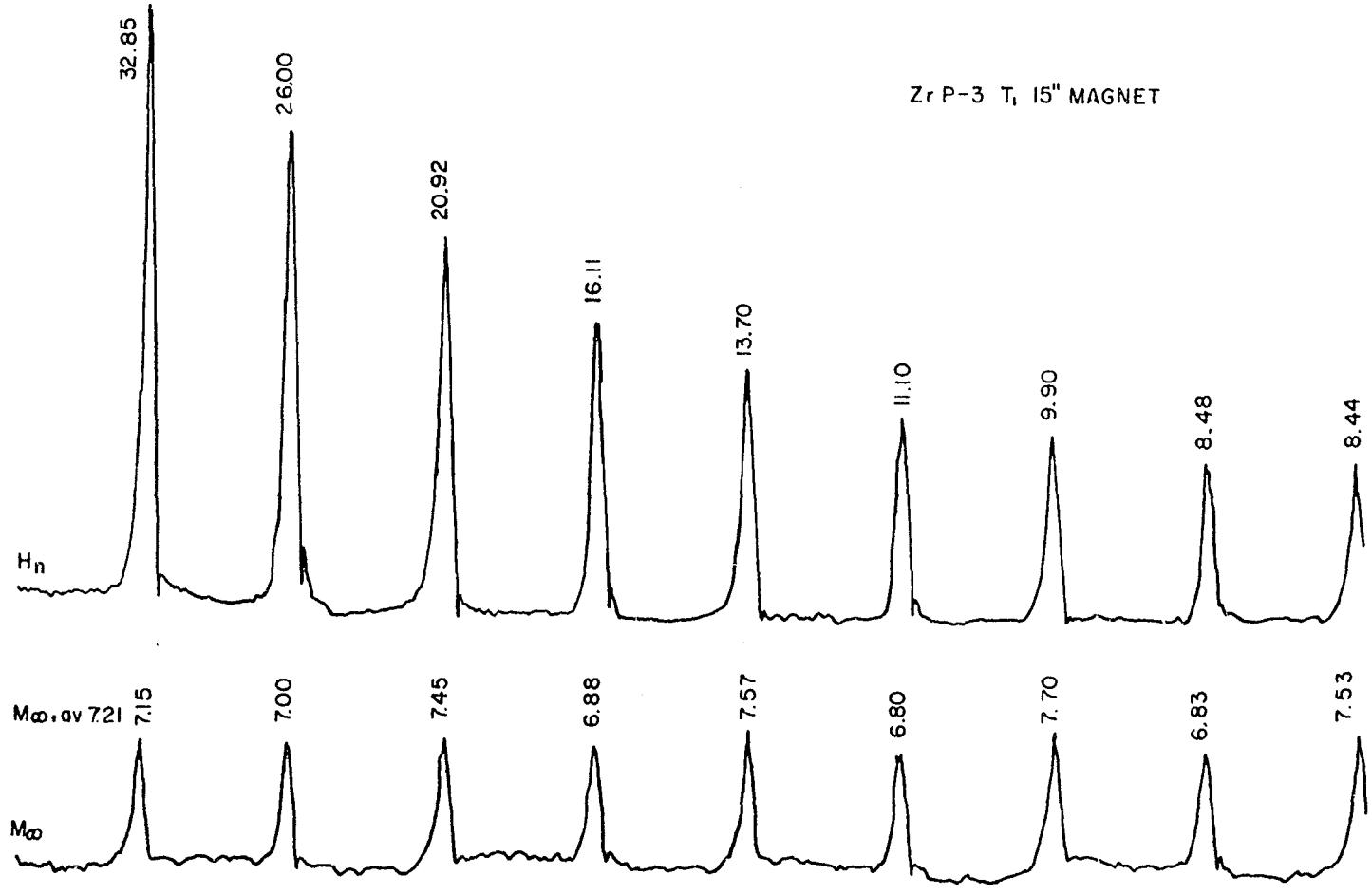

Figure 10. A sample trace for the determination of the spin-lattice relaxation time by the method of tone-burst modulation (see the text of Appendix A for an explanation)

I, of this plot, T_1 is calculated using the equation

$$\frac{\tau}{T_1} = \ln\left[\frac{1 + M_\infty \exp(-I)}{1 + M \exp(S-I)}\right] \qquad (15)$$

where $\tau = (2\nu_m)^{-1}$ and ν_m is the frequency of the modulating triangle wave. Figure 10 represents the data taken at room temperature for ZrP-3 (Zr_3P). For this run a modulating frequency of 110.9 Hz was used. Each scan was 0.04 sec in duration followed by a 0.5 sec delay. The summation time including the delay was 10 min. An operating frequency of 16.008707 MHz was used. Intensities are reported in arbitrary units above each peak, and the average value of M_∞ was used in the calculation of T_1 as well as in the $\ln(H_n - M_\infty)$ vs $\underline{n}$ plot. The method of least squares was used to determine I and S.